Fraunhofer
IAPT

FRAUNHOFER RESEARCH INSTITUTION FOR ADDITIVE MANUFACTURING TECHNOLOGIES IAPT

ALLIANCE DEEP DIVE | 2021

EXCLUSIVE

COST EFFECTIVE POWDERS FOR LBM

ADDITIVE
ALLIANCE

1_ABSTRACT

COST EFFECTIVE POWDERS FOR LBM

Overview of current powder production, costs and processing of coarse TiAl6V4

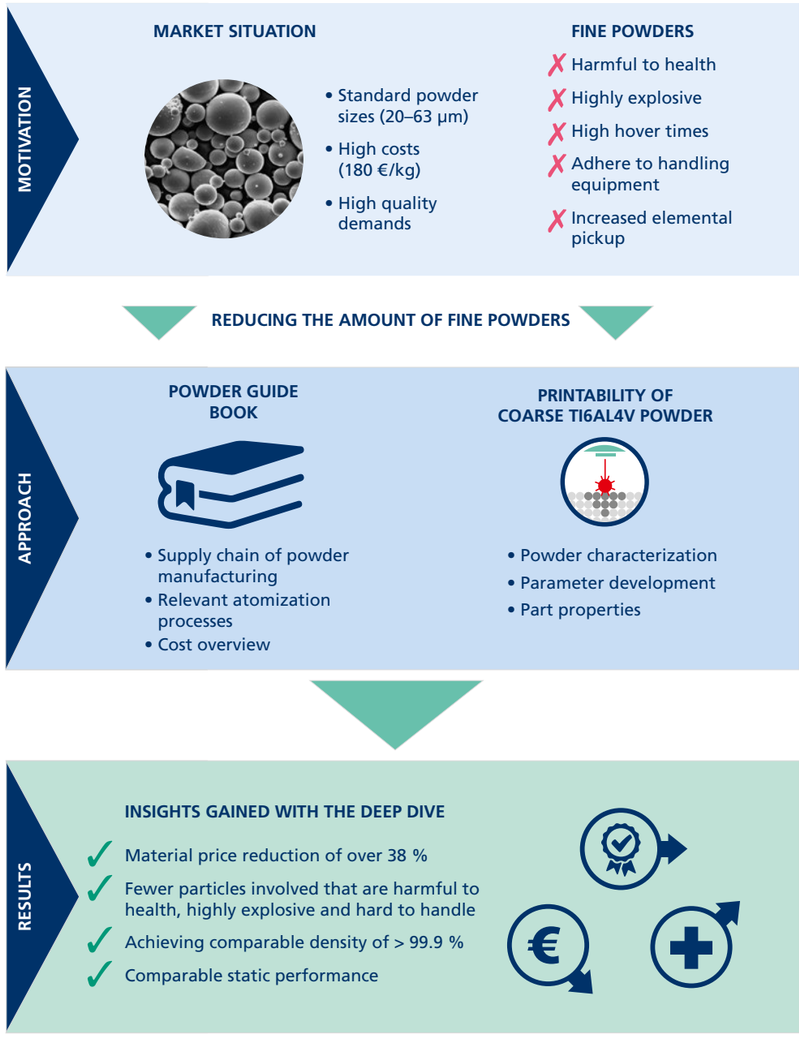

Contact

Fraunhofer Research Institution for
Additive Manufacturing Technologies IAPT

Am Schleusengraben 14
21029 Hamburg-Bergedorf
Germany

Telephone +49 40 48 40 10-500

info@iapt.fraunhofer.de

www.iapt.fraunhofer.de

www.linkedin.com/company/fraunhofer-iapt

www.youtube.com/FraunhoferIAPT

2_CONTENT

3_ACKNOWLEDGEMENT

Deep Dives are reports intended exclusively for the members of the Additive Alliance®. They provide latest insights into the science behind additive manufacturing (AM). Our gratitude goes to the following members. This Deep Dive could not have been prepared without their financial support.

3D SYSTEMS · aalberts surface technologies · Additive Industries
AIRBUS · ALTAIR · BeAM an AddUp company
BIONIC PRODUCTION · DB · DMG MORI
EOS · FANUC · FFT
GE Additive · HHLA HAMBURGER HAFEN UND LOGISTIK AG · HEXAGON simufact
H&H · PREMIUM AEROTEC · RENISHAW apply innovation™
SIEMENS · SIGMA LABS · SLM SOLUTIONS
stratasys · toolcraft · YXLON

formnext

Mesago Messe Frankfurt, organizer of the Formnext, has been the official sponsor and cooperation partner of the Additive Alliance® and the Fraunhofer IAPT since 2020.

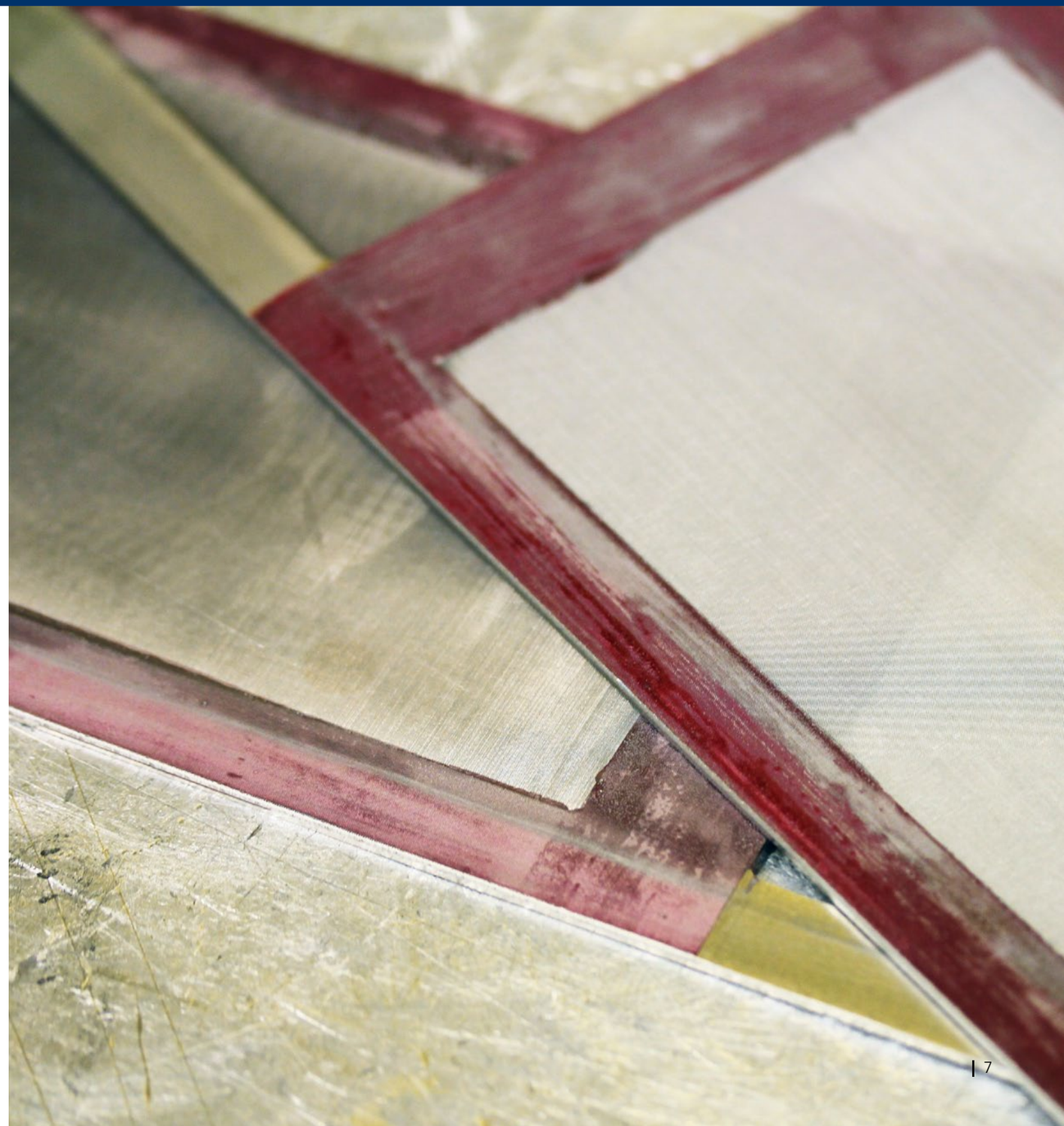

4_ABOUT THE AUTHORS

The authors of this Deep Dive want to contribute to more sustainable, robust and economical metal powder usage in AM. Combining many years of research experience in metal powders for laser powder bed fusion (LB-PBF), they aim to provide detailed know-how, demonstrate new possibilities for particle size distribution (PSD) modifications with the example of coarse powder and enable hitherto unseen cost reduction potential along the AM process chain. In addition, they are constantly trying to enable safer and more efficient powder handling with new ideas and guidelines.

Maximilian Kluge, *M.Sc.*
Head of Materials and Finish

Ina Ludwig, *M.Sc.*
Project Manager

Please do not hesitate to contact our team with any questions:

Maximilian Kluge
Telephone +49 40 48 40 10-728
maximilian.kluge@iapt.fraunhofer.de
https://www.iapt.fraunhofer.de/de/kompetenzbereiche/am-process.html

5_MOTIVATION

Constant developments in powder production have shown that it is possible to produce high-quality powders in large quantities for LB-PBF. When the search for suitable powder specifications began, there was great correspondence between the PSD and the layer thicknesses used in the AM process, so that technical advances in AM also led to constant adjustments of the requested powder characteristics. Recent years have seen successful definitions of powder standards that lead to high densities and good mechanical properties of the parts, establishing typical PSDs such as 20–63 µm.

Stipulating powder characteristics enables greater process stability, but current developments also show that more and more productive manufacturing parameters are being devised, often with high layer thicknesses of over 60 µm and thus also offering space to adapt the powder specifications even further [1].

There are two decisive factors behind the idea of working with coarser powder. On the one hand, there is **resource efficiency.** Only a certain proportion of the produced powder can be used as LB-PBF powder. In the case of a 20–63 µm distribution, the fractions < 20 µm and > 63 µm are mainly declared as rejects or, at best, can be used by other product lines. It can be assumed that the wider the required PSD, the more efficient the use of the powder output for the LB-PBF process.

The other important factor is the proportion of **fine powder** in the distribution. Fine particles have strong interparticle forces, tend to become electrically charged and therefore adhere to the powder handling equipment. Besides the adhesiveness, fine particles can easily be blown away and have high hover times in the air. The finer the particles, the more likely they are to enter the alveoli of human lungs so that skin contact and inhalation of powder constitute potential health risks. Fine particles also enhance the pyrophoric characteristics of the powder; due to their higher specific surface, they form explosive dust atmospheres more easily.

With these disadvantages of fine and narrow powder in mind, this Deep Dive advocates the processing of coarser and wider PSDs, choosing Ti6Al4V as one of the most established AM materials and investigating the influences on part quality and overall powder costs.

INSIGHTS TO BE GAINED:

- Technical overview of relevant atomization processes, typical PSDs and powder qualities
- Powder-related cost indications
- Mechanical and physical properties of additively manufactured parts using coarse Ti6Al4V powder

6_APPROACH OF THE DEEP DIVE

6.1_POWDER GUIDE BOOK

To get an understanding of powder qualities, the Powder Guide Book gives an overview of the powder production process chain, presenting the most common atomization processes and indicating the powder costs (Figure 1).

Both powder quality and production costs are important key factors in powder production. The two factors are determined by the powder production supply chain. This Deep Dive therefore presents the single steps in the production road, starting with the input material, followed by atomization and classification, and ending with certification.

The atomization process defines the particle morphology such as particle shape, size and surface as well as the final chemical composition. There are many processes that differ according to rod material, melting technique and nozzle system. This Guide Book presents the most common atomization techniques for AM as essential know-how.

In addition a market survey was conducted to indicate the cost reduction potential. Prices were compared for a commonly used PSD of 20–63 µm and coarse distributions around 45–105 µm. Quantities of 100 kg and 1 t were quoted to consider economies of scale.

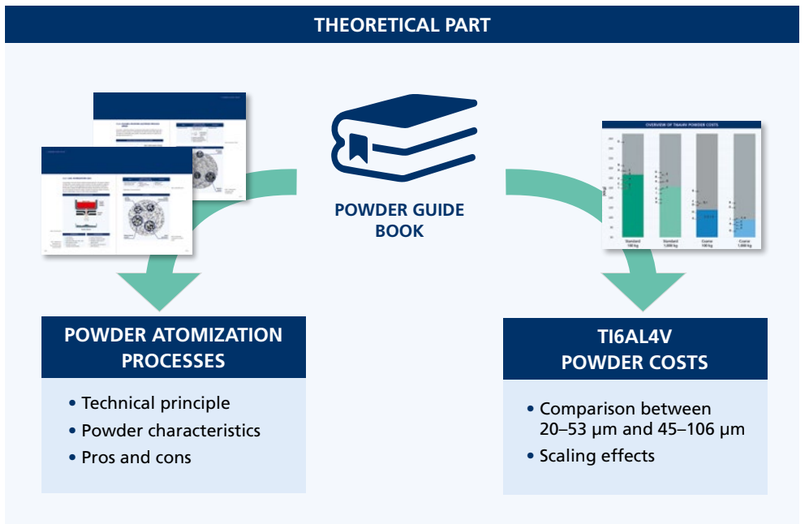

Figure 1: Approach of the Powder Guide Book

6.2_PRINTABILITY OF COARSE TI6AL4V POWDER

For the experimental part of the Deep Dive, the Ti6Al4V alloy was chosen as one of the most relevant and established AM materials on the market. This titanium alloy is characterized by an excellent density-to-strength ratio. Its lightweight and biocompatibility properties make it an ideal choice in many current applications. The downside of the alloy is its rather high material price. One kilogram of Ti6Al4V costs around three to five times more than a typical AM aluminum alloy such as AlSi10Mg. Reducing the material cost of titanium powder is therefore especially relevant for reducing the overall manufacturing cost.

For the investigations, a PSD of 45–106 µm was processed using the LB-PBF process. Compared to a current standard of 20–63 µm, this powder shows a much wider PSD and a significantly lower amount of fine powders as well as a fairly decent price reduction of approximately 38–44 %.

In order to characterize the powder, PSD, morphology and flowability properties were measured before the material was processed on both an SLM250 HL and a Concept Laser M2 machine. A parameter study was carried out to identify suitable process parameters. Tensile specimens and density cubes were produced for further material characterization. Porosity, hardness, surface roughness and tensile properties were chosen as the evaluation criteria to assess the quality of the resulting parts after heat treatment.

The experimental part (graphic overview shown in Figure 2) is intended to serve as an indication of whether the choice of an inexpensive powder variant also means compromising on quality, while at the same time showing the cost reduction potential of working with coarser PSDs.

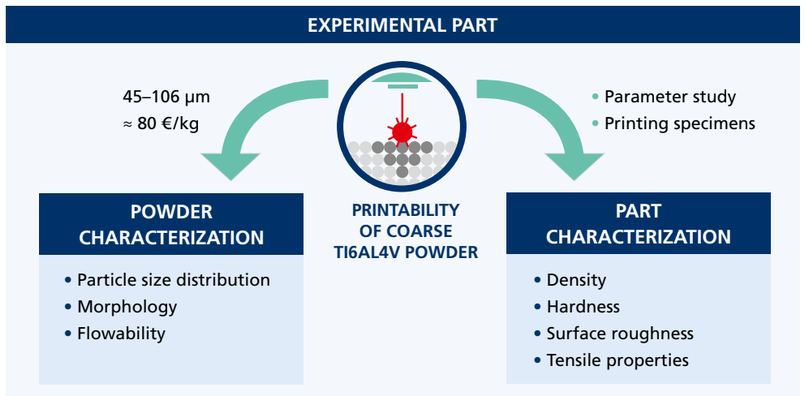

Figure 2: Approach of the experimental part

7_POWDER GUIDE BOOK

7.1_SUPPLY CHAIN OF POWDER MANUFACTURING

The following Figure 3 shows a typical supply chain from the raw material to the qualified AM powder. Cost saving potential can be identified on the basis of the single process steps, e.g. classification for using coarse powders.

INPUT MATERIALS

- Rod
- Sponge
- Wire
- Scrap

ATOMIZATION

Most common atomization processes for Ti6Al4V powders:

- Gas atomization (GA)
- Water atomization (WA)
- Electrode induction melting inert gas atomization (EIGA)
- Plasma atomization (PA)
- Plasma rotating electrode process (PREP)

CLASSIFICATION

- Separation of whole particle size range into PSDs with defined size limits
- Sieving for upper size limit
- Air classifier to separate fine particles

CERTIFICATION

- Different qualities: grade 5 and grade 23
- Testing of relevant powder characteristics such as PSD, morphology, chemical composition, flowability, etc.

Figure 3: Powder supply chain [2]

7.2_RELEVANT ATOMIZATION PROCESSES

Several processes for atomizing metal powders are suitable for AM. They differ in their use of raw material, nozzle technology and atomization medium. The following chapter presents the four most relevant processes for producing titanium powder [3]:

GAS ATOMIZATION (GA)	ELECTRODE INDUCTION MELTING INERT GAS ATOMIZATION (EIGA)
PLASMA ATOMIZATION (PA)	PLASMA ROTATING ELECTRODE PROCESS (PREP)

GA is one of the most used processes for industrial atomization. EIGA and PA are widely used for atomization due to their good chemical control. WA for example is not suitable for reactive materials and therefore excluded. PREP, on the other hand, is a niche process for producing highly spherical particles and is thus also considered in this Deep Dive [4].

7.2.1_GAS ATOMIZATION (GA)

Gas atomization is the most common method for powder production. The material is melted in a crucible within a vacuum chamber as shown in Figure 4. The melt is poured into a high-pressure jet of air, water or inert gas (depending on the specific process) and atomized. The drops fall freely inside a chamber and solidify before being collected. During free fall, the surface tension of the metal pulls the drop into a sphere. To protect the metal from oxidation, the atomizing gas is usually nitrogen or argon, but other variants are possible [6;7].

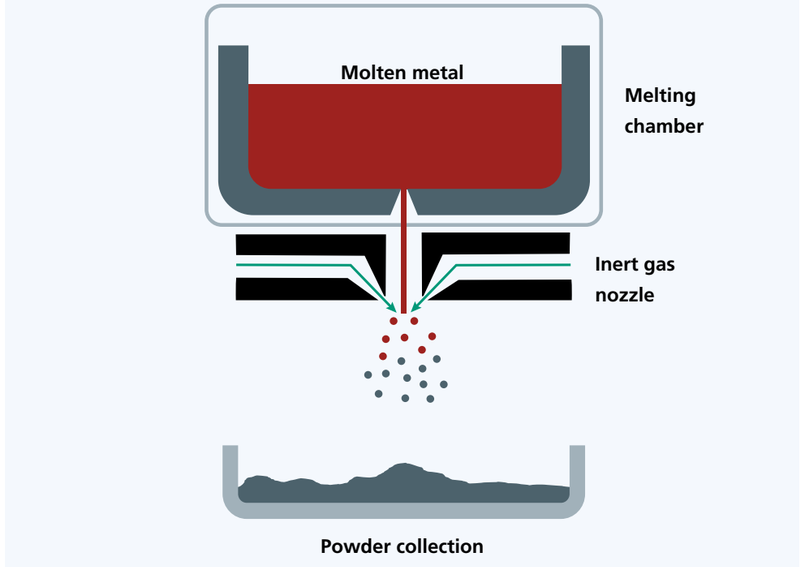

Figure 4: GA process [4;5]

ADVANTAGES	DISADVANTAGES
✓ Cost efficient	✗ Variety of particle forms
✓ Fast production	✗ Impurities caused by crucible
✓ Production variety (GA, VIGA*, WA)	✗ Possibility of argon pores in bigger particles
✓ Wide selection of alloys	✗ Few suppliers atomize titanium with this process
✓ Scalable technology: very high volumes available	

*Table 1: Advantages and disadvantages of GA, *Vacuum induction melting inert gas atomization*

INPUT	MORPHOLOGY AND PARTICLE DISTRIBUTION	MATERIALS
• Raw material, semi-finished products (ingots, scrap metal, metal rods, etc.)	• Spherical • Tendency to form asymmetrical particles • 0–500 µm*	• Meltable metals • Mostly used: Ni, Co, Fe, Al, Cu

Table 2: Characteristics of GA

* depending on process parameters

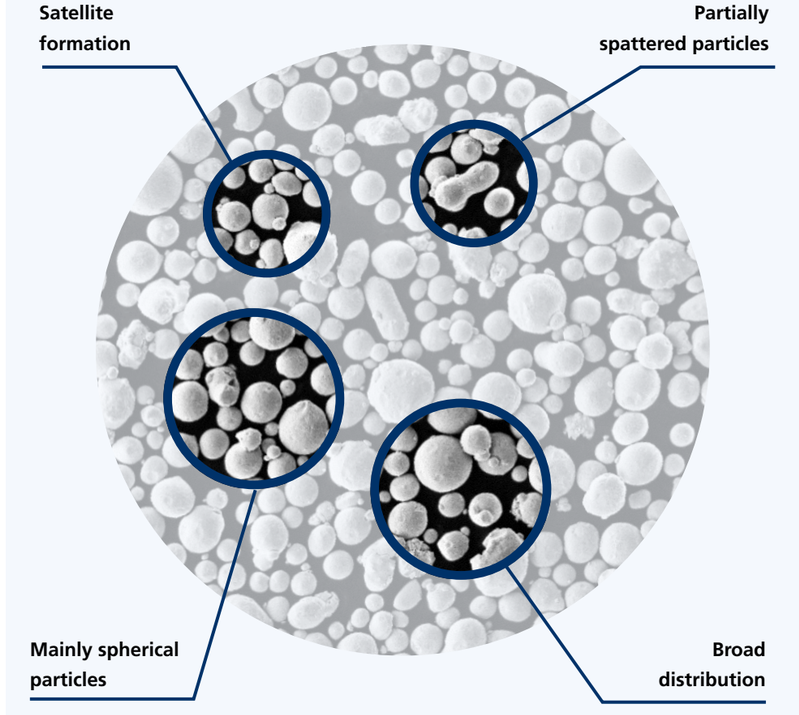

Figure 5: Typical powder morphology of GA atomized powder

7.2.2_ELECTRODE INDUCTION MELTING INERT GAS ATOMIZATION (EIGA)

Electrode induction melting inert gas atomization (EIGA) is presented in Figure 6. The material in form of a rod electrode rotates between the induction coil and under the protection of vacuum or inert gas. The electrode is inductively and continuously melted in the absence of a crucible. The melt falls into a high pressure jet of inert gas and atomizes. The drops fall freely inside a chamber and solidify before being collected. The feedstock is not in contact with a crucible or any other medium, thus greatly limiting the possibility of pollution [9].

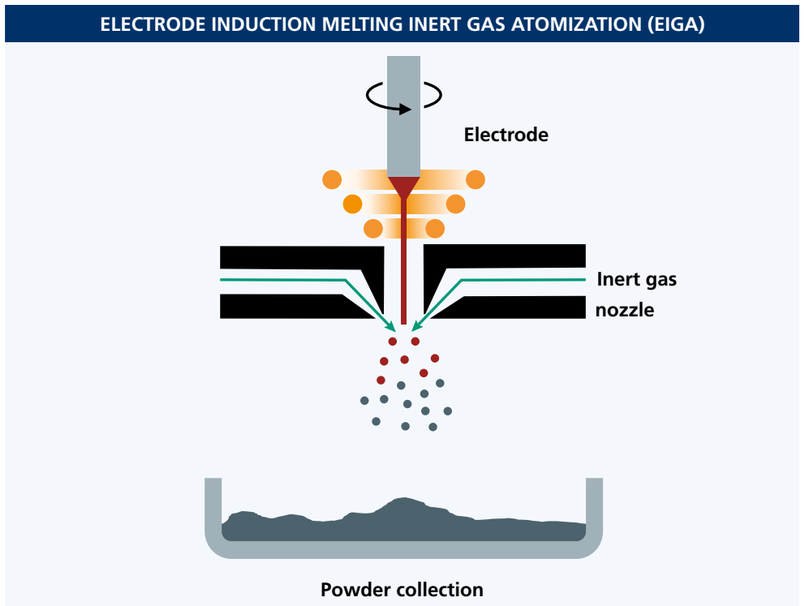

Figure 6: EIGA process [4;8]

ADVANTAGES	DISADVANTAGES
✓ High chemical purity	✗ Expensive
✓ Mostly spherical particles	✗ Input as rod electrodes
✓ Energy efficient	✗ Possibility of argon pores in bigger particles
✓ Particularly suitable for highly reactive materials	✗ Limited by feedstock

Table 3: Advantages and disadvantages of EIGA

INPUT	MORPHOLOGY AND PARTICLE DISTRIBUTION	MATERIALS
• Rod electrode Ø25–70 mm	• Spherical • Slight tendency to form asymmetrical particles • 0–500 µm*	• Reactive and meltable metals • Mostly used: Al, Fe, Mg, W, Mo, Ni, Ti, Cu

Table 4: Characteristics of EIGA

* depending on process parameters

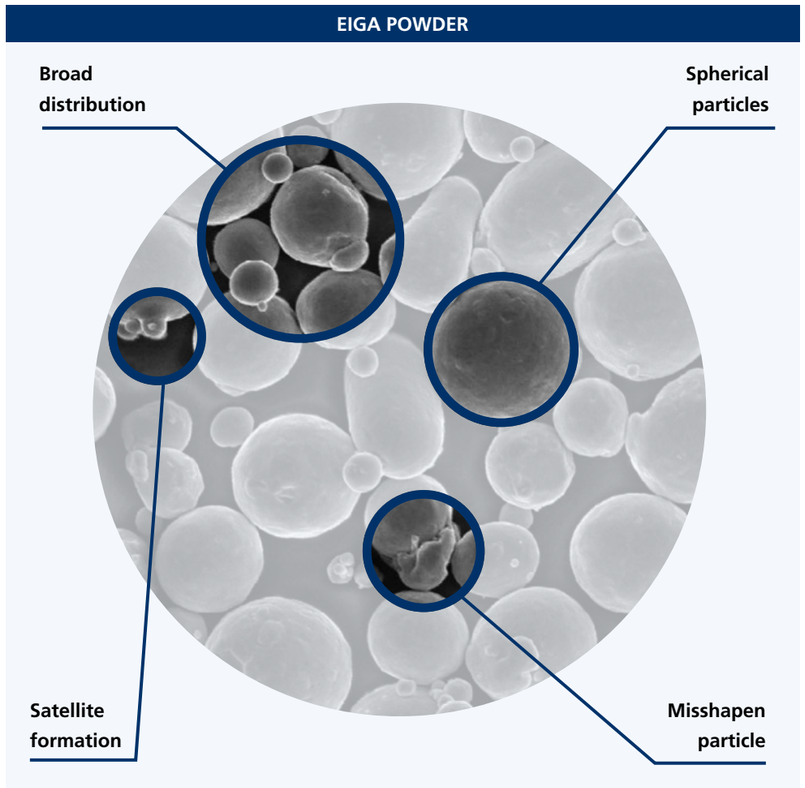

Figure 7: Typical powder morphology of EIGA atomized powder

7.2.3_PLASMA ATOMIZATION (PA)

The material in the form of a wire is inserted into a chamber (Figure 8). A high amount of energy is applied so that the gas (usually helium) ionizes and creates a plasma. The plasma hits the wire at high velocity, causing atomization of the material. The particles are cooled and then collected. The process creates very spherical particles with excellent flow rate. The main challenge with plasma atomization is the high manufacturing cost due to limited production rates and low alloy flexibility, as the material has to be available as as thin wire. Plasma is also used for plasma spherodization (ICPS), a finishing step to spherodize irregularly shaped particles [7;10;12].

PLASMA ATOMIZATION (PA)

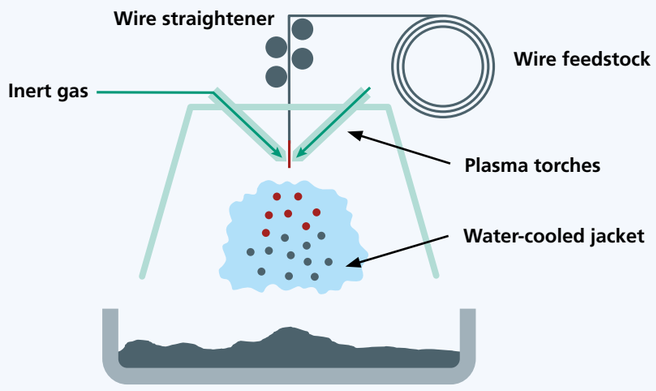

Figure 8: PA process [4;11]

ADVANTAGES	DISADVANTAGES
✓ High chemical purity	✗ Expensive
✓ Very spherical particles	✗ Input as thin wire
✓ Low argon consumption	✗ Possibility of argon pores in bigger particles
✓ Particularly suitable for highly reactive materials	✗ Limited by feedstock
✓ Titanium alloys available	

Table 5: Advantages and disadvantages of PA

INPUT	MORPHOLOGY AND PARTICLE DISTRIBUTION	MATERIALS
• Wire Ø~3 mm	• Mainly spherical • 0–250 µm*	• Reactive and meltable metals • Mostly used: Ti, Ni, Zr, Mo, Nb, Ta

Table 6: Characteristics of PA

* depending on process parameters

PA POWDER

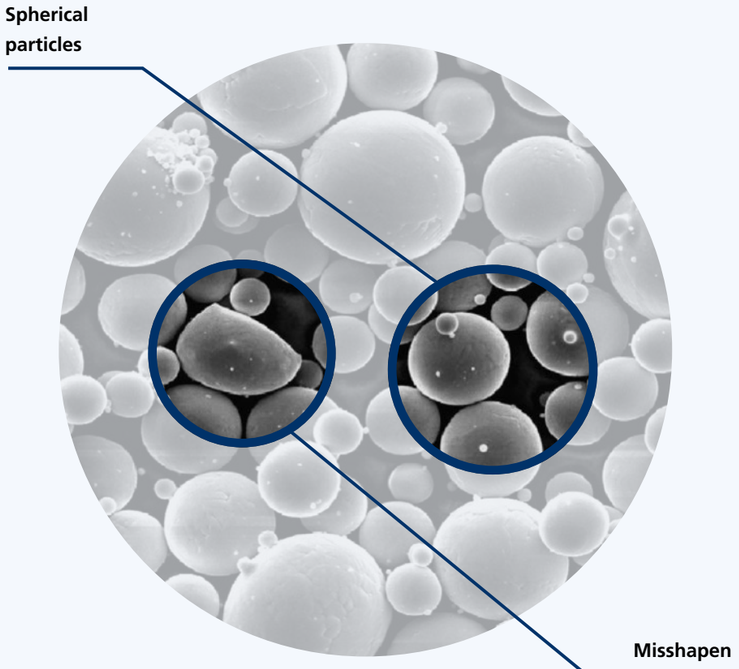

Figure 9: Typical powder morphology of PA atomized powder

7.2.4_PLASMA ROTATING ELETRODE PROCESS (PREP)

The powder is produced by rotating a rod electrode at high speed and melting the end with a plasma arc as shown in Figure 10. Centrifugal force then ejects the liquid metal radially, forming droplets that solidify before being collected. The powder particles are very spherical and have high chemical purity [7;13].

PLASMA ROTATING ELECTRODE PROCESS (PREP)

Figure 10: PREP process [4;12]

ADVANTAGES	DISADVANTAGES
✓ Low scattering of particle size	✗ High energy consumption
✓ Very spherical particles	✗ Input as rod
✓ Low argon consumption	✗ Not completely fluid before atomization (anisotropic particles)
✓ Few argon pores in bigger particles	✗ Limited by feedstock
✓ Titanium alloys available	

Table 7: Advantages and disadvantages of PREP

INPUT	MORPHOLOGY AND PARTICLE DISTRIBUTION	MATERIALS
• Electrode Ø~64 mm	• Highly dependent on process parameters: $d = \frac{k}{\omega}\sqrt{\frac{\Upsilon}{\rho D}}$ ω: rotating speed ϒ: surface tension of the liquid metal D: diameter of the electrode ρ: density of the molten metal k: empirical constant between the value of 2.67 and 6.55	• Meltable metals

Table 8: Characteristics of PREP

PREP POWDER

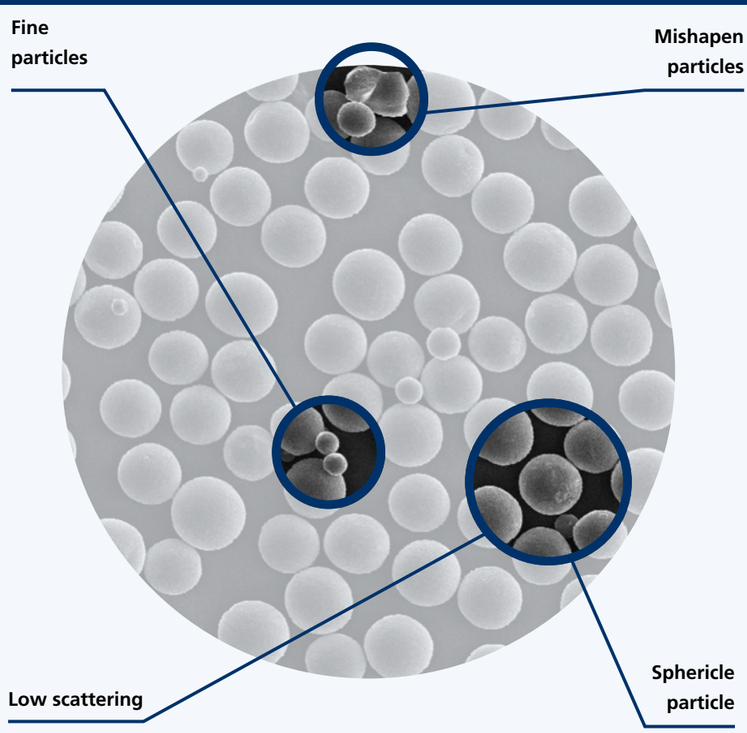

Figure 11: Typical powder morphology of PREP atomized powder

7.3_COST OVERVIEW

To obtain a representative overview of what Ti6Al4V powders cost on the market, quotations were obtained from a total of 22 suppliers, of which 15 responded with an official offer. Four suppliers were declared as outliers, so that the database of 11 suppliers was analyzed. In order to evaluate the influencing factor of purchase quantity and PSD, the following standardized requirements were sent to all suppliers:

Powder: Ti6Al4V ELI (grade 23)
PSD: 20–63 µm and 45–106 µm
Quantities: 100 kg and 1,000 kg

The survey included manufacturers and traders, but no AM machine manufacturer. The suppliers participating in the survey used different production processes that have not been explicitly assigned. Any currency conversions were carried out on September 2, 2021. No price negotiations were held with any of the suppliers. The offers were obtained in the period from June 1 to August 31, 2021. The quotation from the supplier providing the powder for the experiments in chapter 8.2 was not included in this survey.

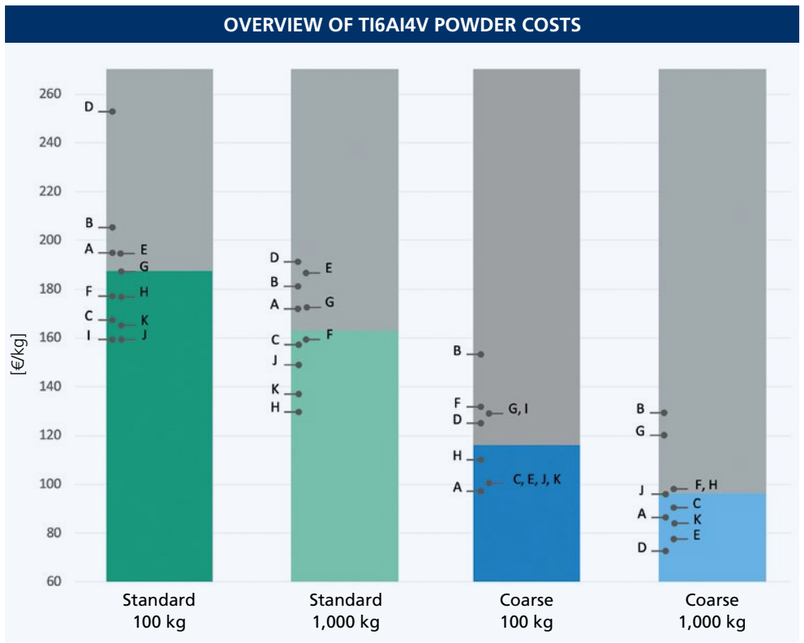

Figure 12: Comparison of standard and coarse Ti6Al4V powder costs, A–K = Different suppliers

Figure 12 shows 4 bars, each representing a combination of PSD and a specific quantity. The reference distribution is declared as "standard", as the suppliers offered a variety of PSDs such as 15–53 µm or 20–63 µm. The coarser distributions are declared as "coarse" and also in this case a variety of slightly differing PSDs were offered such as 44–106 µm, 45–100 µm or 45–125 µm. The upper end of the colored area indicates the mean values of the individual powder variants.

A look at the results reveals clear trends. On the one hand, the order volume leads to significant scaling effects, with the choice of a coarser PSD triggering even larger cost reduction effects. On the basis of the 11 offers considered, it emerged that increasing the order volume from 100 to 1,000 kg reduced the price of the standard PSD by an average of 12 %. Similar and even greater effects were seen on selecting an increased order volume of the coarse powders. Due to volume scaling, the offered price was on average 19 % lower.

In comparison to the standard, an average of 38 % of the costs could be saved by choosing a coarse powder for an order quantity of 100 kg, increasing to an average of 44 % for 1,000 kg.

The following prices were achieved by considering only the most competitive provider in each segment (Figure 13).

Figure 13: Prices of the cheapest provider in each segment

These numbers clearly show that significant cost reductions can be achieved by selecting coarse powders in large volumes, and that a broad variety of suppliers can fulfill these requirements. In some cases the coarse powders are also listed as EBM or LMD powders and are often standardized powder fractions that are provided by most suppliers.

8_PRINTABILITY OF COARSE TI6AL4V POWDER

8.1_POWDER SPECIFICATION

The material used in this Deep Dive is a Ti6Al4V powder purchased with the quality level ELI, grade 23 in a 45–106 µm PSD. The initial powder price was 80 €/kg, but 90 kg of powder were then bought for 30 €/kg due to a sales promotion. The supplier's inspection certificate shows the following chemical composition in Table 9 [14]:

	TI (WT%)	AL (WT%)	V (WT%)	FE (WT%)	C (WT%)	O (WT%)
45–106 µm powder	Balance	6.15	4.0	0.15	0.01	0.08
Nom. ELI	Balance	5.5 – 6.5	3.5 – 4.5	≤0.25	≤0.08	≤0.13

Table 9: Chemical composition measured by the supplier with ICP-OES, CA and IGF

Particle morphology

The PSD and the particle shape were measured by dynamic image analysis (according to ISO 13233-2) [15] using the Camsizer X2 from Microtrac Retsch GmbH and compared in Table 10 to the diffraction stated by the supplier [16] and a reference powder 20–53 µm Ti6Al4V.

	D10 [µm]	D50 [µm]	D90 [µm]	SPHT	SYM-METRY	B/L
Measured by supplier with laser diffraction	46.20	69.45	102.45	/	/	/
45–106 µm measured with dynamic image analysis	51.93	71.23	92.13	0.885	0.926	0.859
20–53 µm measured with dynamic image analysis	22.17	33.47	46.83	0.895	0.954	0.896

Table 10: Compared particle size distribution: Laser diffraction (supplier) vs. dynamic image analysis (IAPT)

The PSD is stated with the particle size at a determined value of the cumulative distribution. For example, the D50 value indicates that 50 % of all particles in the sample are less than or equal to the D50 value. The PSD is also shown in Figure 14. The PSD values given by the powder supplier are confirmed overall, even though the measurements taken by the authors show a slightly narrower distribution. This gap is explained by the different measurement techniques that were used. The morphology is defined by sphericity (roundness, calculated from the particle circumference and the particle area), symmetry (smallest resulting radius ratio) and aspect ratio (width/length ratio). The morphology of the 45–106 µm powder is marginally less spherical than the 20–53 µm powder.

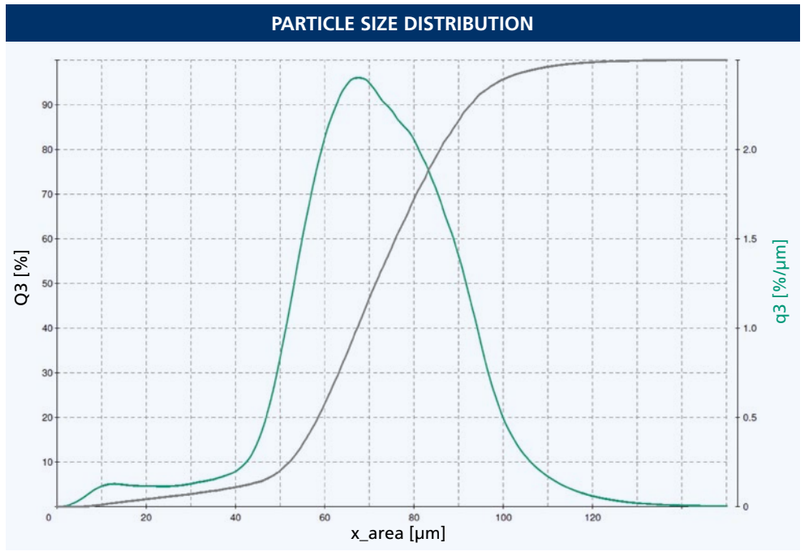

Figure 14: Particle size distribution

Flowability

Bulk density and tapped density were measured using a Hall Flowmeter according to ISO 3923-1 [17] and ISO 3953 [18]. Flowability is described by the Hauser ratio, the ratio of tapped to bulk density $H = \rho_t/\rho_b$ and the time required for 50 g powder to pass the Hall Flowmeter [19]. The 45–106 µm powder is compared to a typical 20–53 µm Eli Ti6Al4V powder shown in Table 11.

POWDER	BULK DENSITY [g/cm³]	TAPPED DENSITY [g/cm³]	HAUSNER RATIO	FLOWABILITY [s/50g]
20–53 µm	2.46 +/- 0.00	2.68 +/- 0.01	1.09	26.75
45–106 µm	2.30 +/- 0.01	2.53 +/- 0.01	1.10	25.20

Table 11: Flowability measured via Hall Flow

To determine flowability with greater precision, the avalanche angle and the cohesion were measured with the Granudrum by Granutools. The Granudrum has a glass-sided rotating drum filled with 50 ml of powder. For each rotating speed, the avalanche angle α is calculated from the average interfacial position (Figure 15) and the dynamic cohesion index σ (Figure 16) is measured from the interfacial fluctuations. Rotating speed increases from 2 up to 55 rpm and decreases again [20].

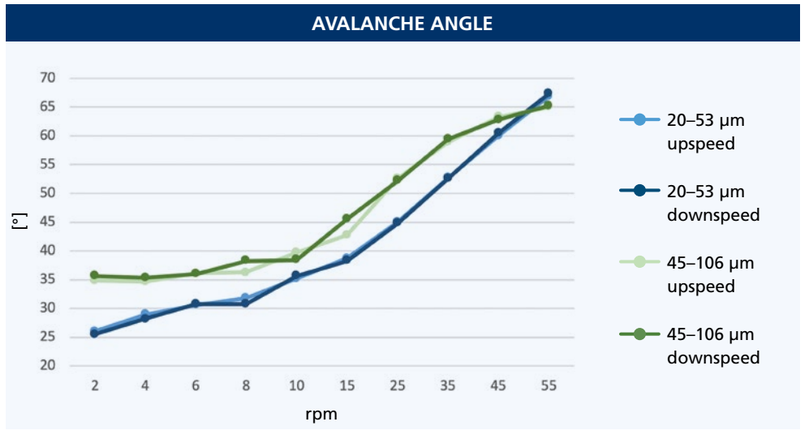

Figure 15: Avalanche angle of 20–53 µm and 45–106 µm powders

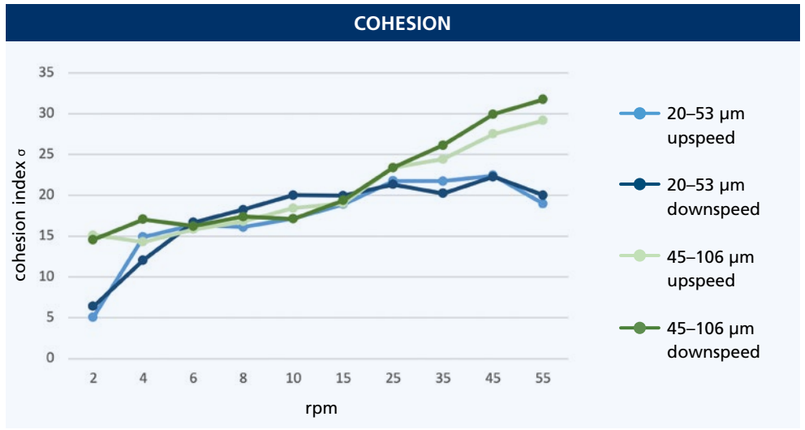

Figure 16: Cohesion of 20–53 µm and 45–106 µm powders

Decreasing flowability at increasing rotating speed leads to shear-thickening rheological behavior in all powders. The coarse powder shows similar adaptation to rotating speed as the standard powder, with slightly reduced overall flowability

8.2_EXPERIMENTS

The experimental part aims to show the cost reduction potential of coarser 45–106 µm powder with the development of a suitable parameter set. Cubes were therefore printed to optimize the process parameters for the value density. Initial attempts were carried out on an SLM 250 HL and the final parameter set was developed on a Concept Laser M2.
For each print job, 36 cubes were placed on the building platform as shown in Figure 17. In the first print job each cube was printed with a different parameter set to determine the process window. 108 cubes were printed and analyzed on the Concept Laser M2 LB-PBF machine.

DENSITY CUBE POSITIONS

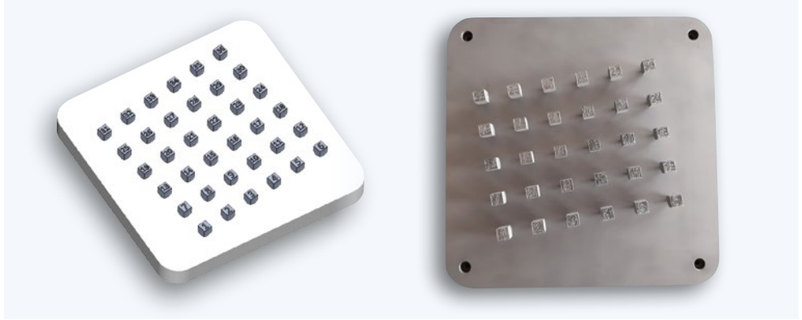

Figure 17: Typical image of density cube positions on the build plate – CAD and image

Design of experiments

For all iterations, the layer thickness was set to 60 µm and the laser spot had a diameter of 100 µm. The machine has two integrated 400 W lasers, of which only one was used to generate the specimens. The building platform was not (pre-)heated.

A suitable parameter set was identified by varying laser power, scanning speed and hatch distance. The following factors and levels shown in Table 12 were initially used for full factorial design of experiment (DoE)

P_L [W]	v_s [mm/s]	Δy_s [µm]
320	1,000	100
340	1,100	110
360	1,200	120
-	1,300	-

Table 12: Factors and levels for parameter development

On reaching a density of more than 99.9 % within the density cubes, the best nine parameter sets were chosen and validated four times. The best parameter set was fixed as final parameter set (Table 13) and used to produce the tensile specimens.

Layer thickness [µm]	60	**Contour power [W]**	300
Power [W]	320	**Contour scanning speed [mm/s]**	1,000
Scanning speed [mm/s]	1,400	**Contour hatch distance [µm]**	100
Hatch distance [µm]	80	**Build rate [cm³/h]**	24.14

Table 13: Final parameter set

For the build job of the final test specimens, the form B d_0 = 5 mm according to DIN 50125 [21] was produced 12 times: 6 times with a vertical angle of 0° and 6 times with a horizontal angle of 90°, with an offset of 1 mm. 6 density cubes were also manufactured as illustrated in Figure 18. Both the tensile specimens and the density cubes (one excluded as reference) were heat treated at 800 °C for 2 hours before being separated from the build plate by wire cut eroding EDM.

FINAL SPECIMENS ON BUILD PLATE

Figure 18: Image of final specimens on the build plate – CAD and image

Parameter development did not include improving the parameters for better surface roughness or subsurface porosity. All tensile specimens were machined before testing the final geometry of the form B d_0 = 5 mm.

MEASURED PROPERTIES

- Density
- Vickers hardness
- Surface roughness

EVALUATED TENSILE PROPERTIES

- Tensile strength R_m
- Yield strength $R_{p0.2}$
- Elongation at break A
- Young's modulus E

8.3_TESTING AND ANALYSIS

8.3.1_Density measurements

The density cubes were hot mounted with a CitroPress by Struers using the polymeric matrix ClaroFast. Table 14 shows the progressive grinding steps to obtain a scratch-free polished surface.

POLISH STEP	FORCE
MD Piano 80	25 N
SiC Foil #180	20 N
SiC Foil #320	20 N
SiC Foil #800	15 N
SiC Foil #1200	15 N
SiC Foil #2000	10 N
SiC Foil #4000	10 N
MD Chem – OP-U	20 N

Table 14: Grinding and polishing program

Images were taken with a digital microscope VHX-5000 by Keyence using 50x magnification and dark-field illumination. Multiple images were merged for one specimen. Density was calculated with software based on the region of interest (ROI) using a threshold of 125 [-].

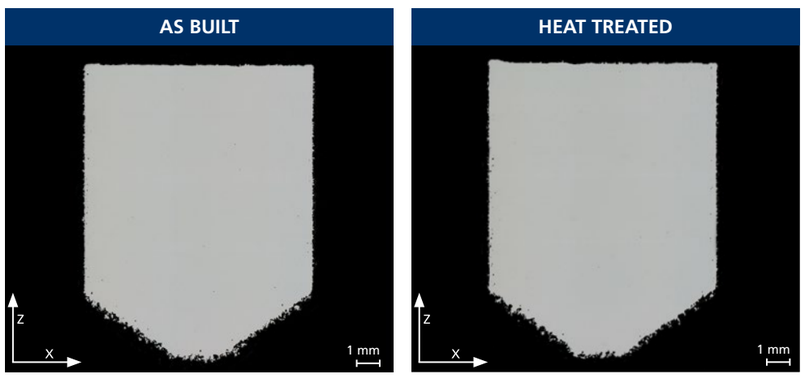

Figure 19: Polished surface of density cube as built and heat treated

The final parameter set produced mean density values of 99.92 % as shown in Figure 19. The contour and down skin parameters were not optimized so that these aspects were not taken into account. Density with the 45–106 µm powder is moderately lower than with the standard powder. Typical values are between 99.90–100 % (EOS, SLM, GE) [22-24].

8.3.2_Hardness measurements

Hardness was measured on the polished density cubes with a DuraScan by Struers according to ISO 6507-1 [25]. Vickers hardness was measured using a four-sided diamond pyramid with a square base, an angle of 136° and a load of 10 kgf (98 N). HV10 hardness was measured on each cube at three spots and the mean value was taken.

One cube was not heat treated to show the influence of stress relief treatment on specimen hardness. The hardness values of the heat treated cubes are within the range stated by the machine supplier [22-24] as shown in Figure 20, though slightly higher than the average/mean hardness.

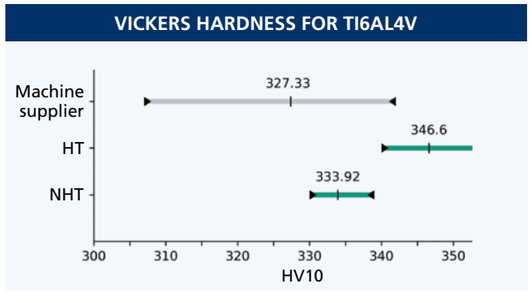

Figure 20: Vickers hardness for Ti6Al4V

minimum *maximum* | *mean*

8.3.3_Surface roughnesss

Surface roughness was measured and analyzed according to DIN EN ISO 25178 [26] using a 3D laser scanning confocal microscope VK-8710 by Keyence. Three points in all spatial directions were defined and scanned to create a three-dimensional scan of the surface. A scan field of 529.9 x 706.6 µm was measured with a 20x lens and a lateral measurement resolution of 0.345 µm.

The target values consist of the surface roughness parameters Sa for arithmetic mean height Sa and Sz for maximum height Sz, both calculated using an S-L surface.

S-filter: 2 µm
L-filter: 0.5 mm

The surface roughness data stated in the datasheets provided by the machine suppliers [22-24] show Ra values between 7 and 18 µm (Figure 21). It must be said that Ra and Sa are barely comparable. Previous investigations by IAPT (Surface Studies) showed that it is possible to expect as-built values of approximately 17 µm Sa for parts made of Ti6Al4V. As already mentioned, the investigations of this Deep Dive did not include any optimization of the surface or contour parameters so that there is a corresponding gap in quality.

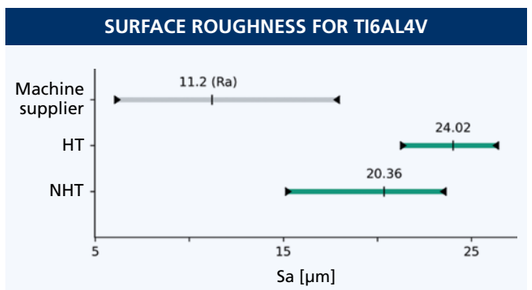

Figure 21: Surface roughness for Ti6Al4V

minimum *maximum* | *mean*

8.3.4_Tensile properties

Tensile specimens were tested to compare the static mechanical properties of parts built using coarse powder with parts manufactured using standard powder. The specimen design was therefore chosen according to DIN 50125 [21] with form B and diameter d_0 = 5 mm as illustrated in Figure 22. The specimens were produced with a 1 mm xy-offset and a 2 mm z-offset and subsequently machined to the final testing geometry. The tensile tests were performed according to DIN EN ISO 6892-1 [27] with a Galdabini – Quesar 600 kN (maximum load) at 20 °C. The results are compared to the material datasheets of LB-PBF machine suppliers [22-24] evaluated for 60 µm layer thickness process parameters and heat treated specimens.

The following parameters were determined:

- Tensile strength R_m [N/mm²]
- Yield strength $R_{p0.2}$ [N/mm²]
- Elongation at break A [%]
- Young's modulus E [N/mm²]

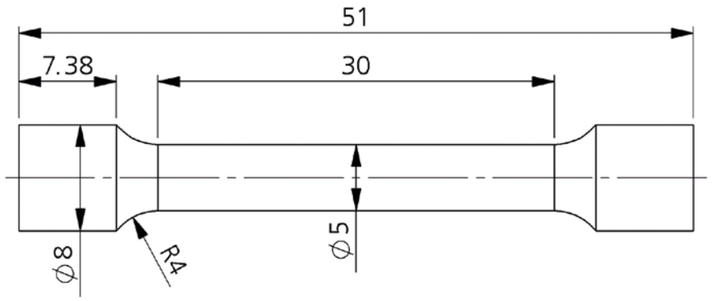

Figure 22: Tensile specimen form B with d_0 = 5 mm acc. to DIN 50125

VERTICAL 0°	R_m [MPa]	$R_{p0.2}$ [MPa]	A [%]	E [GPa]
IAPT 45–106 µm (M2 Cusing 60 µm/400 W)	1,018.2	906	17.92	116
EOS (EOSINT M 280-400 W; EOS M 290-400 W)	1,100	1,000	14.5	110
SLM (60 µm/400 W)	991	905	15	130
GE (Laser M2 Series 5; 60 µm)	1,050	995	14.5	119

Table 15: Tensile test results for the vertical specimen

Table 15 shows the results of tensile testing for the vertical 0° specimens. Tensile strength, yield strength and Young's modulus for the 45–106 µm powder are slightly lower than the results of the machine suppliers. In contrast, the results for elongation at break are significantly higher with almost 18 %.

HORIZONTAL 90°	R_m [MPa]	$R_{p0.2}$ [MPa]	A [%]	E [GPa]
IAPT 45–106 µm (M2 Cusing 60 µm/400 W)	1,051	955	14.62	118
EOS (EOSINT M 280-400 W; EOS M 290-400 W)	1,100	1,000	13.5	110
SLM (60 µm/400 W)	987	894	12	112
GE (Laser M2 Series 5; 60 µm)	1,050	995	13.5	118

Table 16: Tensile test results for the horizontal specimen

The results for the horizontal 90° specimen are similar to the results for the vertical specimens, as indicated in Table 16. Tensile strength and yield strength are slightly lower than the average reference, in contrast to the higher values for Young's modulus and elongation at break as well as better ductility.

Overall, the 45–106 µm powder reaches comparable results with strength that is slightly lower but still high and with improved ductility.

9_SUMMARY & CONCLUSION

This Deep Dive is divided into two parts: the Powder Guide Book, and the investigations into the processability of coarse Ti6Al4V powder.

The Powder Guide Book gives an overview of the supply chain of metal powder production together with the most common AM atomization processes for titanium, indicating the differences within the various atomization processes and potential cost levers along the supply chain. Based on a survey of 22 powder suppliers, consideration was given to 11 offers for 20–63 µm and 45–106 µm powders for order volumes of 100 kg and 1,000 kg. Scaling effects show an average price decrease of 12 % for the standard powders and 19 % for the coarse powders. Choosing a coarse powder instead of the standard resulted in average cost savings of 38 % for an order quantity of 100 kg and even 44 % for 1,000 kg. This demonstrates a significant correlation between the powder price and the order quantity as well as the PSD.

After demonstrating the cost reduction potential of the 45–106 µm powder, the focus then turned to processability. The powder was analyzed and compared to a standard distribution of 20–53 µm. The sphericity, apparent and tapped density of the 45–106 µm powder were slightly lower. The Hausner Ratio and the flow rate through the funnel also demonstrated a decreased performance. Shear thickening behavior was measured in both powders using a Granudrum. The 45–106 µm powder showed a greater increase in cohesion than the 20–53 µm powder. Both had good results, with the 20–53 µm powder performing marginally better overall.

As part of a parameter study, the values for laser power, scanning speed and hatch distance were optimized on an SLM 250 HL and a Concept Laser M2. The final parameter set was developed on the Concept Laser M2 using a 100 µm laser spot diameter and a 60 µm layer thickness. The final build rate was at 24.14 cm^3/h. 6 density cubes, 6 vertical and 6 horizontal tensile specimens were produced using the identified parameter set. The parts were tested after heat treatment at 800 °C for 2 hours.

The mean density of 99.92 % was just slightly lower than the values achieved by machine suppliers with standard powder. It was not possible to identify any differences in hardness. In view of the fact that the contour parameters were not optimized, the surface roughness values (Sa) were remarkably lower compared to machine suppliers' and internal reference data.

The static mechanical properties showed a slight decrease in strength for both vertical and horizontal specimens, while elongation at break was 22 % higher than the mean value of the comparative specimens.

To summarize, it can be stated that modifications towards a coarser PSD show high future potential. According to the experiments, choosing an inexpensive powder variant means no significant compromise in terms of quality and even indicates an improvement with regard to ductility. At the same time, it was possible to demonstrate the cost reduction potential and lowering health risks by selecting coarser PSDs.

Outlook

Further investigations could cover higher productivity rates and therefore higher layer thicknesses. It is still necessary to adapt the contour and downskin parameters for the 45–106 µm powder. Further research is needed into the influence of a coarser PSD on the static and dynamic mechanical properties of additively manufactured parts as well as the influence on other materials in order to confirm the results of the Deep Dive and to reveal the cost reduction potential of the individual alloys.

10_REFERENCES

[1] Seyda, V. (2018). Werkstoff- und Prozessverhalten von Metallpulvern in der laseradditiven Fertigung. https://doi.org/10.1007/978-3-662-58233-6.

[2] Dawes, J., Bowerman, R. & Trepleton, R. (2015). Introduction to the Additive Manufacturing Powder Metallurgy Supply Chain. *Johnson Matthey Technol Rev* 59, 243–256. https://doi.org/10.1595/205651315X688686.

[3] Kassym, K. & Perveen, A. (2020). Atomization Processes of Metal Powders for 3D Printing. *Materials Today: Proceedings* 26, 1727–1733. https://doi.org/10.1016/j.matpr.2020.02.364.

[4] Ebel, T., Ferri, O. M., Limberg, W. & Schimansky, F.-P. (2011). Metal Injection Molding of Advanced Titanium Alloys. *Advances in Powder Metallurgy & Particulate Materials*, Proceedings of the International Conference on Powder Metallurgy & Particulate Materials, PowderMet 2011. Vol. 1 San Francisco, CA (USA). 4, 45–57.

[5] Chen, G., Zhao, S. Y., Tan, P., Wang, J., Xiang, C. S. & Tang, H. P. (2018). A Comparative Study of Ti-6Al-4V Powders for Additive Manufacturing by Gas Atomization, Plasma Rotating Electrode Process and Plasma Atomization. *Powder Technology* 333, 38–46. https://doi.org/10.1016/j.powtec.2018.04.013.

[6] Park, S. (2020). Optimization Studies for the Gas Atomization and Selective Laser Melting Processes of Al10SiMg Alloy. *Electronic Theses and Dissertations*, 2020–. 267. https://stars.library.ucf.edu/etd2020/267.

[7] Tingskog, T. (2018). An Introduction to Metal Powders for AM. *Manufacturing Processes and Properties, Metal AM* 4, 111–119.

[8] Sun, P., Fang, Z. Z., Zhang, Y. & Xia, Y. (2017). Review of the Methods for Production of Spherical Ti and Ti Alloy Powder. *JOM* 69, 1853–1860. https://doi.org/10.1007/s11837-017-2513-5.

[9] León, G. P., Lamberti, V. E., Seals, R. D, Abu-Lebdeh, T. M. & Hamoush, S. A. (2016). Gas Atomization of Molten Metal: Part I. Numerical Modeling Conception. *American Journal of Engineering and Applied Sciences* 9, 303–322. https://doi.org/10.3844/ajeassp.2016.303.322.

[10] Vert, R., Pontone, R., Dolbec, R., Dionne, L. & Boulos, M. I. (2016). Induction Plasma Technology Applied to Powder Manufacturing: Example of Titanium-Based Materials. *Key Engineering Materials,* Vol. 704, 282–286¸ doi:10.4028/www.scientific.net/KEM.704.282.

[11] Dodun, O., Tsetkou, A., Papapanos, G., Vardavoulias, M., Nagît, G. & Slătineanu, L. (2007). A Theoretical Equation for the Thermal Balance at Plasma Atomizing Process. *Nonconventional Technologies Review* No.1.

[12] Baskoro, A. S., Supriadi, S. & Dharmanto, D. (2019). Review on Plasma Atomizer Technology for Metal Powder. *MATEC Web Conf.* 269, 5004. https://doi.org/10.1051/matecconf/201926905004.

[13] Tang, J., Nie, Y., Lei, Q. & Li, Y. (2019). Characteristics and Atomization Behavior of Ti-6Al-4V Powder Produced by Plasma Rotating Electrode Process. *Advanced Powder Technology* 30, 2330–2337. https://doi.org/10.1016/j.apt.2019.07.015.

[14] Heraeus Acceptance Test Certificate 3.1, EN 10204/3.1; Powder Ti6Al4V Grade 23, May 21, 2021.

[15] ISO 13233-2. International Organization for Standardization (2006). Particle Size Analysis – Image Analysis Methods –: Part 2: Dynamic Image Analysis Methods. ICS 19.120.

[16] Heraeus Test Certificate PSD; Ti6Al4V, Laser Diffraction. March 24, 2021.

[17] DIN EN ISO 3923-1 (2018). Metallic Powders – Determination of Apparent Density – Part 1: Funnel Method. ICS 77.160, 2018. https://dx.doi.org/10.31030/2823249.

[18] DIN EN ISO 3953 (2011). Metallic Powders – Determination of Tap Density (ISO 3953:2011). German version EN ISO 3953:2011; 2011-05; ICS 77.160. https://dx.doi.org/10.31030/1754956.

[19] ISO 4490. International Organization for Standardization (2018). Metallic Powders – Determination of Flow Rate by Means of a Calibrated Funnel (Hall flowmeter). ICS 77.160.

[20] Granutools Granudrum Operators Guide. Granutools Sprl. Compiled July 2, 2016.

[21] DIN 50125. Standards Committee Materials Testing (2016). Testing of Metallic Materials – Tensile Test Pieces. ICS 77.040.10.

[22] EOS Material Data Sheet, EOS Titanium Ti64. EOS GmbH – Electro Optical Systems. Compiled October 29, 2014, last reviewed August 31, 2011. https://trin.do/wp-content/uploads/2016/07/EOS_Titanium_Ti64_de.pdf.

[23] SLM Material Data Sheet, SLM Ti-Alloy Ti6Al4V ELI (Grade 23) / 3.7165/B348/F136. SLM Solutions Group AG. Compiled October 22, 2020. https://www.slm-solutions.com/fileadmin/Content/Powder/MDS/MDS_Ti-Alloy_Ti6Al4V__ELI_0719.pdf.

[24] GE Material Data Sheet, GE M2 Series 5 Ti6Al4V Grade 23. GE Additive Germany GmbH. Compiled July 27, 2020. https://www.ge.com/additive/sites/default/files/2021-02/M2SERIES5_TI64_CMDS_REV2_120%C2%B5m.pdf.

[25] DIN EN ISO 6507-1 (2018). Metallic Materials – Vickers Hardness Test – Part 1: Test Method (ISO_6507-1:2018). German version.

[26] DIN EN ISO 25178-1 (2016). Geometrical Product Specifications (GPS) – Surface Texture – Areal – Part 1: Indication of Surface Texture. German version.

[27] ISO 6892-1. International Organization for Standardization (2019). Metallic Materials – Tensile Testing – Part 1: Method of Test at Room Temperature. 6th ed. ICS 77.040.10.

Imprint

Fraunhofer Research Institution for
Additive Manufacturing Technologies IAPT
Am Schleusengraben 14
21029 Hamburg-Bergedorf
Germany
Telephone +49 40 48 40 10--500
Fax +49 40 48 40 10--999
www.iapt.fraunhofer.de
info@iapt.fraunhofer.de

A legally dependent entity of
Fraunhofer-Gesellschaft
zur Förderung der angewandten Forschung e.V.
Hansastrasse 27c
80686 Munich
Germany
www.fraunhofer.de
info@zv.fraunhofer.de

Contact

M.Sc. Maximilian Kluge
Head of Materials and Finish
Telephone +49 40 48 40 10-728
maximilian.kluge@iapt.fraunhofer.de

Status of the Deep Dive, October 2021.